ACS APPLIED MATERIALS & INTERFACES

Research Article

www.acsami.org

Fabrication of Biomimetically Patterned Surfaces and Their Application to Probing Plant–Bacteria Interactions

Boce Zhang,[†,‡] Yaguang Luo,[*,†,§] Arne J. Pearlstein,[⊥] Jesse Aplin,[†,‡] Yi Liu,[∥] Gary R. Bauchan,[△] Gregory F. Payne,[∥,#] Qin Wang,[‡] Xiangwu Nou,[†] and Patricia D. Millner[†]

[†]Environmental Microbial and Food Safety Lab, Agricultural Research Service, United States Department of Agriculture, Beltsville, Maryland 20705, United States

[‡]Department of Nutrition and Food Science, University of Maryland, College Park, Maryland 20742, United States

[§]Food Quality Lab, Agricultural Research Service, United States Department of Agriculture, Beltsville, Maryland 20705, United States

[⊥]Department of Mechanical Science and Engineering, University of Illinois at Urbana—Champaign, Urbana, Illinois 61801, United States

[∥]Institute for Bioscience and Biotechnology Research, University of Maryland, College Park, Maryland 20742, United States

[△]Electron and Confocal Microscopy Unit, Agricultural Research Service, United States Department of Agriculture, Beltsville, Maryland 20705, United States

[#]Fischell Department of Bioengineering, University of Maryland, College Park, Maryland 20742, United States

ABSTRACT: We have developed a two-step replica molding method for rapid fabrication of biomimetically patterned plant surfaces (BPS) using polydimethylsiloxane (PDMS-BPS) and agarose (AGAR-BPS). Beyond providing multiple identical specimens that faithfully reproduce leaf surface microstructure, this approach also offers unique chemical, physical, and biological features. PDMS-BPS provide good structural durability for SEM examination, have surface wettability comparable to plant surfaces for coating development, and allow for real-time monitoring of biosynthesis through incorporation into microfluidic devices. AGAR-BPS are compatible with bacterial growth, recovery, and quantification, and enable investigation of the effects of surface topography on spatially varying survival and inactivation of *Escherichia coli* cells during biocide treatment. Further development and application of these biomimetically patterned surfaces to study (and possibly modify) other aspects of plant–bacteria interactions can provide insight into controlling pathogen contamination in a wide range of applications.

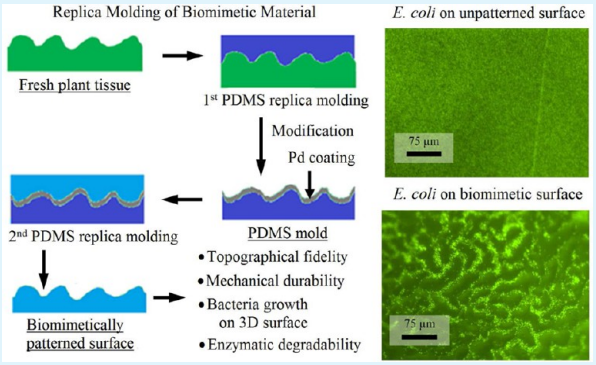

KEYWORDS: *plant–bacteria interaction, biomimetically-patterned surfaces, replica molding, PDMS, agarose, surface topography*

INTRODUCTION

Consumption of pathogen-contaminated food is a major cause of human illness and mortality. The Centers for Disease Control and Prevention (CDC) reports that nearly 48 million illnesses, more than 128 000 hospitalizations, and more than 3000 deaths are attributable to foodborne disease each year in the U.S. alone.[1] Fresh leafy green vegetables (e.g., lettuce, spinach, cabbage) have emerged as a substantial vehicle of foodborne bacterial pathogens, despite use of bactericidal sanitizers (chiefly chlorine) in processing wash water.[2] Evidence strongly indicates that bacterial cells persist to varying degrees on and in tissues of leafy greens. Although internalized contamination originating from seeds and roots is reportedly rare,[3−6] leaves, with their rough and hydrophobic surface microstructures, including stomata, hydathodes, and trichomes, provide protected harborage for bacterial cells in disinfecting/sanitizing washing processes.[3−10]

The importance of surface attachment, and the extent to which local topography and hydrophobicity affect attachment, is evident in the kinetics of bacterial disinfection by chemical sanitizers, where unattached and loosely attached bacteria are easily inactivated, and bacteria strongly attached to a surface are far less vulnerable.[7−9] Unfortunately, the specific mechanisms of attachment/detachment involved in these microscale plant–bacteria surface interactions, and the surface attributes and interfacial forces that affect attachment/detachment, are not understood.[3,7−9] As a result, development of improved mitigation approaches (e.g., involving nonchlorinated sanitizers, surfactants, and ultrasound) is highly empirical.

Received: April 19, 2014
Accepted: July 9, 2014
Published: July 9, 2014

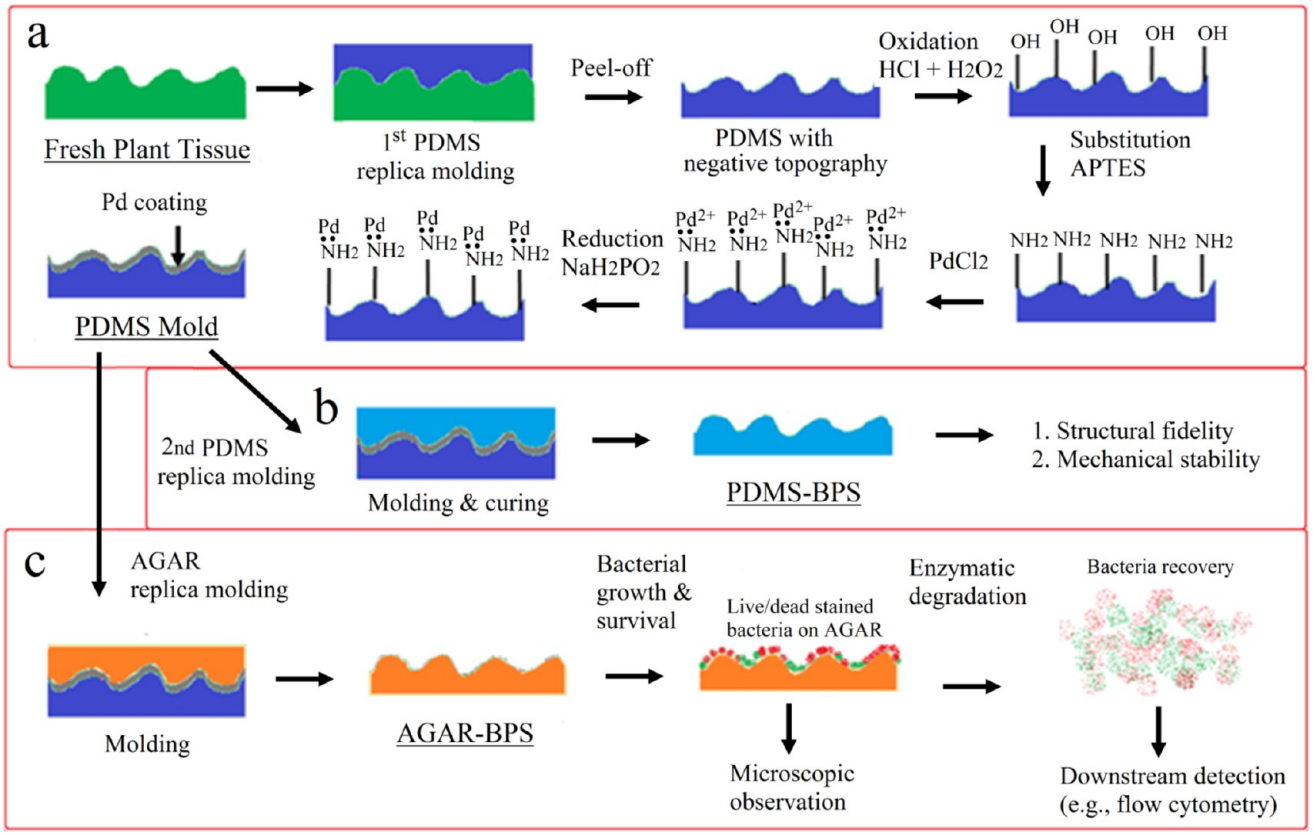

Figure 1. Schematic presentation of BPS fabrication via replica molding: (a) replica molding and chemical modification of Pd-coated PDMS stamp to produce final PDMS mold; (b) thermal molding of PDMS-BPS; (c) thermal molding of AGAR-BPS.

A significant impediment to understanding plant−bacteria surface interactions is that the surface microstructure of leaves varies with species, cultivar, plant, and location on the plant, and is also influenced by growing conditions and maturity stage. These factors make it difficult to replicate experiments, and to interpret variation as a function of experimental parameters. Development of biomimetically patterned surfaces (BPS) that faithfully and reproducibly capture the microstructural topography of plant leaves provides a means to precisely replicate experiments, allowing interpretation of the results when parameters are systematically varied, without confounding influences of natural variation. Moreover, the capability to tailor and characterize surface microstructures (and other surface properties, such as hydrophobicity) will enable experiments that enhance understanding of the interactions between plant surfaces and human pathogens (including those interactions relevant to mitigation strategies), as well as with phytopathogens.

Although artificial surfaces with deliberately patterned micro- or nanoscale texture are frequently used to study attachment, growth, and migration of mammalian cells, a recent review[11] mentions very few previous reports on the use of reproducible surfaces in studies of microbial attachment. Apoga et al.[12] studied appressorial attachment of fungal germlings to regular arrays of pillars on a silicon substrate, as a function of pillar area, and found that essentially no appressoria were induced below a minimum area of the flat pillar end. Held et al.[13] studied attachment of wild-type and mutant *Neurospora crassa* to unpatterned surfaces in microfluidic channels. De la Fuente et al.[14] used an unpatterned polydimethylsiloxane (PDMS) surface in a microfluidic channel to study attachment of a pathogenic grapevine bacterium, and measured very different detachment forces for wild-type and mutant organisms. Finally, Sirinutsomboon et al.[15] used microfabricated silicon surfaces to study attachment of *Escherichia coli* to trichome and stomatal-like structures, and grooves between epidermal cells. Each 2 cm square Si specimen had a spatially periodic array of only one of these features, and each feature type had a geometrically simple topography. These authors found strong localization of attached bacteria at the bases of the trichome-like structures. For the stomatal-like structures, bacteria localized much more strongly at a certain "stand-off" distance (i.e., neither close to nor far from the "stomata"), whereas for grooves no localization was observed.

In none of this work was the surface hydrophobicity, the nanoscale texture, or any other surface property (other than the microscale topography) varied. The capability to simultaneously control microscale topography and surface properties like hydrophobicity, on a reproducible surface, provides the opportunity to examine plant−bacteria surface interactions relevant to food sanitization, including how attachment and detachment are impacted by environmental matrices.

In the present work, we move beyond the previous use of surfaces having simple, highly ordered microstructures with a high degree of symmetry.[16] We first demonstrate that replica-molding using rapid fabrication techniques (Figure 1) produces PDMS- and agarose-based (AGAR) biomimetically patterned surfaces (BPS) having the microstructural topography of a spinach leaf. In addition to microstructural fidelity, we show that these PDMS-BPS have sufficient mechanical integrity under vacuum conditions to allow for electron microscopy. We also demonstrate that PDMS-BPS have surface wettability

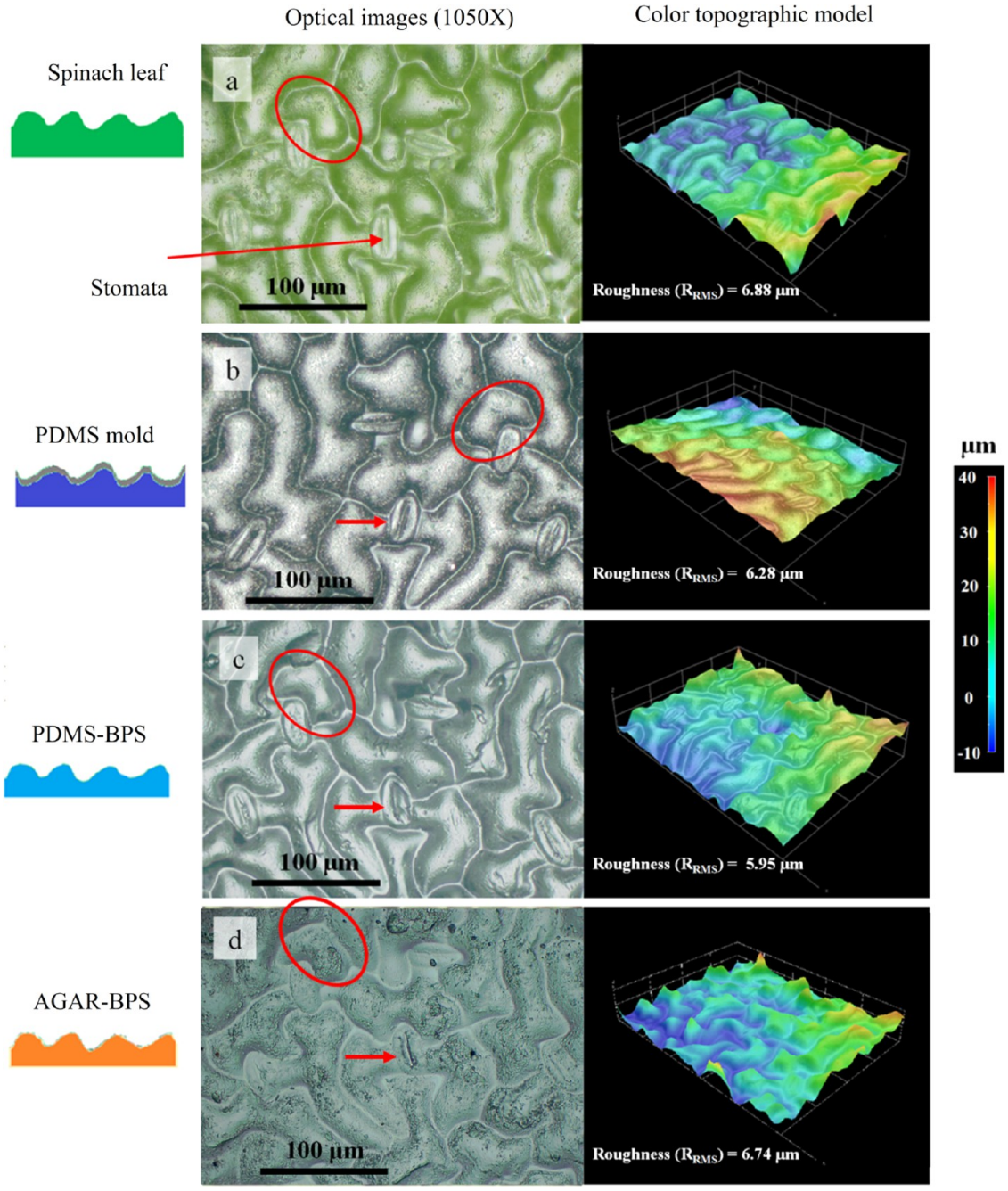

Figure 2. Hirox 3D microscopy images and 3D topographical models show faithful replication of surface topography. (a) Spinach leaf; (b) Pd-coated PDMS stamp; (c) PDMS-BPS; (d) AGAR-BPS. Red circles and arrow highlight the near-identical plant cell morphology, and stomatal structure, respectively, on the surfaces.

characteristics comparable to those of a natural plant tissue, which will aid in the conduct of replicable studies involving the interaction of surface properties and microstructure. Finally, we show that AGAR-BPS with added nutrients provide the capability to study growth and survival of bacteria on a topographically structured surface, and explore the possibility of recovering live and dead bacterial cells via enzymatic degradation and flow cytometry.

RESULTS AND DISCUSSION

Microstructural Characterization of PDMS Stamps and Biomimetically Patterned Surfaces. After preparation of these artificial surfaces, as described in Materials and Methods, it was important to establish that they faithfully reproduced the surface topography of spinach leaves. A Hirox 3D microscope was used to perform 3D imaging of these surfaces. Figure 2 shows optical images and color topographic renderings of (a) the original spinach leaf, and the corresponding areas of (b) the final Pd-coated PDMS stamp (hereinafter referred to as the PDMS mold), (c) the PDMS-BPS, and (d) the AGAR-BPS. The PDMS mold in Figure 2b showed structure and topography mirroring (i.e., opposite to that of) the spinach leaf (Figure 2a). Panels c and d in Figure 2 show the PDMS-BPS and AGAR-BPS replicas of the leaf, respectively, made using the PDMS mold. They are mirror images of the PDMS mold, and clearly provide true replicas of

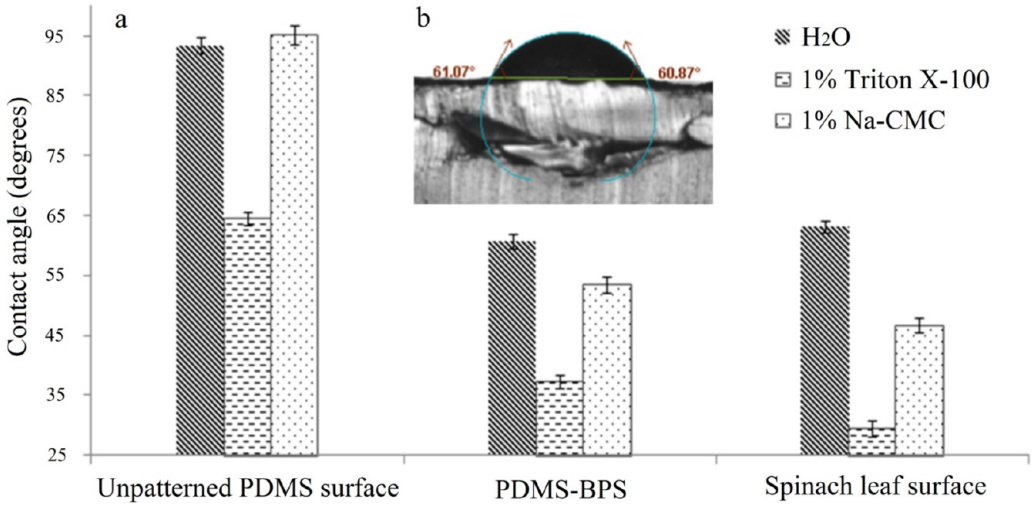

Figure 3. Surface wettability of unpatterned PDMS, PDMS-BPS, and spinach leaf surface for surfactant and coating development. (a) Contact angle measurement (mean ± standard deviation) of water, 1% aqueous solution of Triton X-100, and 1% aqueous solution of Na-CMC. (b) Snapshot of contact angle measurement using sessile drop method (e.g., water on PDMS-BPS).

the surface topographical features (e.g., valleys between built-up cellular structures, etc.) of the original spinach leaf (Figure 2a). These images suggest that surface microstructures of epithelial cells were faithfully reproduced via replica molding. The root-mean-square roughness (R_{RMS}) of the surfaces (examples of which are shown in Figure 2) was measured using the standard deviation of the z-values of all pixels (1.92 million pixels over an area of 300 μm by 200 μm). The results are quite similar for all four surface types, consistent with the hypothesis that, at this resolution, the topographies of the real leaf and of the PDMS and AGAR biomimetically patterned surfaces, are very similar. Much of the variation of R_{RMS} among the different surfaces can be attributed to glare on a glossy surface (e.g., through large apparent peaks or depressions at the edges of the images); and environmental humidity, which can also affect leaf plumpness and the AGAR-BPS surfaces because of either saturation or dehydration.

Wettability of PDMS Biomimetically Patterned Surfaces. PDMS offers the possibility of altering surface physical characteristics while maintaining durable mechanical and transparent optical properties, thus providing insight into plant−bacteria interaction. We first evaluated the potential of PDMS-BPS for in vitro study of plant−bacteria interaction in terms of the potential to provide surface wettability comparable to the natural plant tissue surface, and structural stability in vacuum (VP-SEM).

The surface wettability of spinach leaf, unpatterned PDMS, and PDMS-BPS was evaluated by contact angle measurement on static sessile drops using an optical tensiometer. The inset image in Figure 3 shows contact angles of water, aqueous solutions of Triton X-100 (a nonionic surfactant), and Na-CMC (sodium carboxymethylcellulose, a cellulosic gum used as an edible coating material, thickener, and emulsion stabilizer) on these solid surfaces. We can identify three possible contributors to variance in the contact angle measurements: (a) contact angle hysteresis, in which the measured contact angle of a static drop might differ according to whether the interface has most recently advanced or receded; (b) random or systematic experimental error, including error associated with measurement precision, electronics, vibration, temperature variation, etc.; and (c) for the patterned surfaces, precise location of the drop on the surface. The fact that the variance is small for each combination of surface and liquid suggests that contact angle hysteresis is not very important for any of these combinations, and that small variations in drop position on the patterned surface and leaf are not important for those cases.

The unpatterned PDMS surface was hydrophobic to water and to the Na-CMC solution, with contact angles near 90°. Triton X-100 improves the surface wettability of hydrophobic surfaces by reducing the contact angle to 65°, consistent with previous work.[17] Compared to unpatterned PDMS, biomimetically patterned PDMS surfaces showed much better wettability (corresponding to reductions of 32, 42, and 43% for water, Triton X-100, and Na-CMC, respectively) for drops of all three liquids, probably due to the Cassie impregnating wetting state (the "petal" effect, in which liquid wets large but not small grooves, where adhesive forces between the liquid and solid are very high),[18−20] and the formation of air pockets in the valleys between asperities. For these three liquids, the considerably smaller differences between the wettability of PDMS-BPS and that of spinach leaf (about 5, 12, and 22% for water, Triton X-100, and NaCMC, respectively) show the importance of topography, and suggest significant potential for use of biomimetically patterned surfaces of PDMS in rapid screening of surfactants and coating materials of interest in applications. The ability to replicate different leaf microstructures provides the capability to better understand how topographical features of real biological materials affect wettability. Since both surface biochemistry and topography are critical to bacterial attachment, growth, and inactivation, the present approach allows for a relatively "clean" separation of the effects of surface microstructure from those of surface chemistry and nanoscale texturing. Independent control of the chemical composition and properties of the polymeric surface, while maintaining identical microstructures in the replica-molding process, will be the next step.

SEM Compatibility of PDMS Biomimetically Patterned Surfaces. Because studies of surface topography and structure using SEM and other imaging technologies typically require a high-vacuum environment, we evaluated the structural stability of PDMS-BPS under vacuum conditions in a variable-pressure SEM (VP-SEM). The SEM images indicate that PDMS-BPS

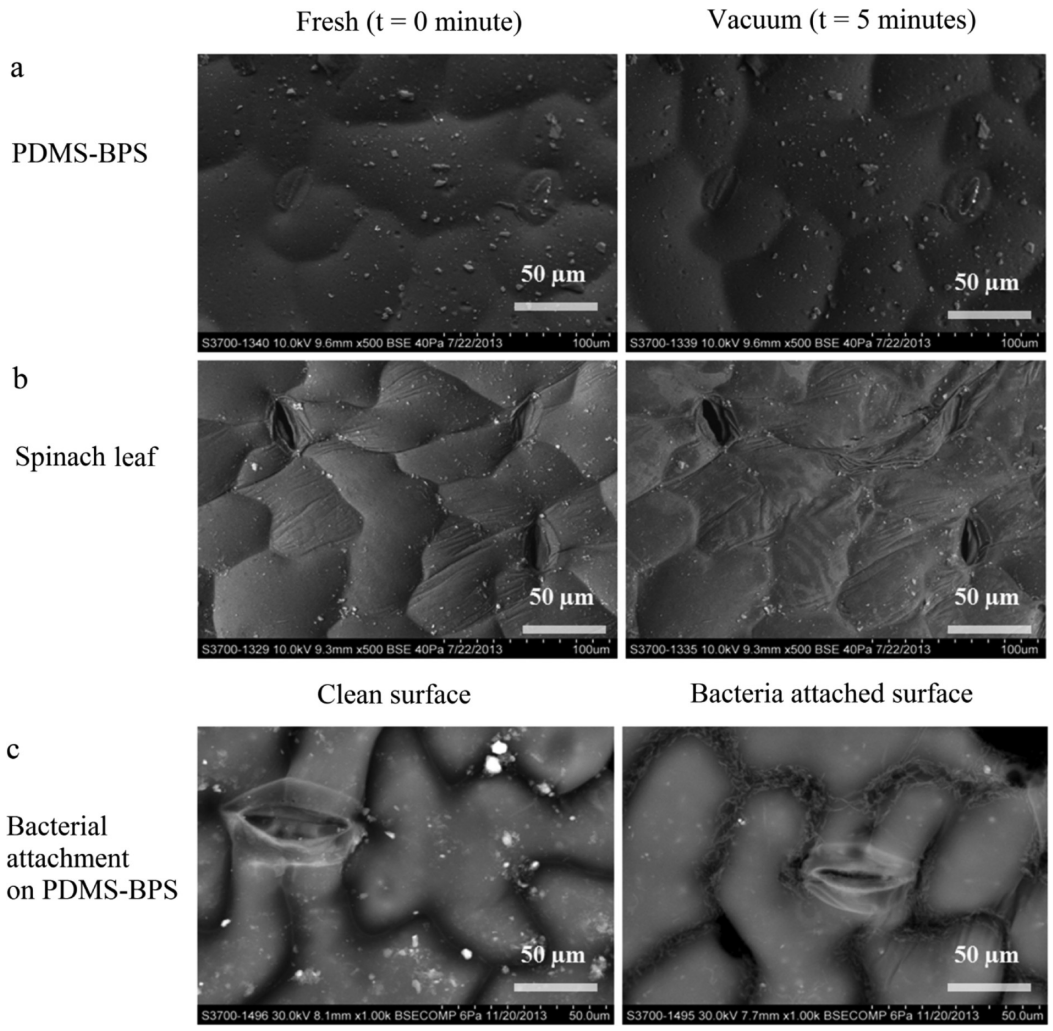

Figure 4. VP-SEM images (500×, −25.0 °C, and 10.0 kV): (a) PDMS-BPS; (b) spinach leaf. Results show that at 40 Pa vacuum, PDMS-BPS is structurally more stable than spinach leaf. (c) Effect of natural topography on bacterial attachment for PDMS-BPS.

(Figure 4a) were robust and very durable in the VP-SEM, and that all topographic features were preserved during vacuum exposure, while the epithelial cells of actual spinach leaf (Figure 4b) collapsed after 5 min at low (40 Pa) vacuum.

The SEM compatibility of PDMS-BPS was used to investigate bacterial attachment, and to provide insight into how natural topography affects bacterial distribution on plant surfaces. Figure 4c shows that bacterial cells tend to concentrate in valleys. This result suggests that the solution in which bacteria are suspended can provide sufficient wetting, despite the hydrophobic nature of both the PDMS surface and the natural spinach tissues. Therefore, transition to the Cassie impregnating wetting state could explain how an aqueous bacterial suspension interacts with natural topography on plant surfaces.[21] The in vacuo stability of the PDMS-BPS strongly suggests that such surfaces can be a valuable tool for detailed SEM examination of plant surface topography, by significantly shortening and simplifying sample preparation. Such studies have the potential to provide insight into spatial distributions of bacterial cells on surfaces, and into the physical and chemical mechanisms that lead to nonuniformity.

Bacterial Growth, Aggregation, and Survival on AGAR Biomimetically Patterned Surfaces. Because of high moisture content (~98% by weight), AGAR-BPS are inferior to natural plant tissue in terms of mechanical strength and vacuum stability. However, AGAR-BPS have two major advantages compared to PDMS and natural leaf surfaces. First, when prepared with suitably controlled nutrient mixtures, they can be used to study the effect of natural surface topography on bacterial growth and survival, and to identify interactions between nutrients and topography, using both wild-type and mutant bacteria. Second, when coupled to downstream detection capability, the enzymatic biodegradability of AGAR-BPS can provide unique capabilities to study cellular attachment, detachment, and surface effects on growth.

Traditionally, investigation of biofilm formation and development of control measures are both based on planktonic culture and volume statistics, which do not account for any topographical information, including effects of bacterial localization. However, the current consensus on bacterial biofilms is that surface topography strongly affects bacterial spatial distribution and physiological activities.[8,16,22−25] Modern cellular and molecular technologies (e.g., flow cytometry, PCR, etc.) can provide cellular and molecular level insight into the temporal behavior and ultimately the fate, of individual bacterial cells. To explore these possibilities, we conducted several experiments to identify potential opportunities in

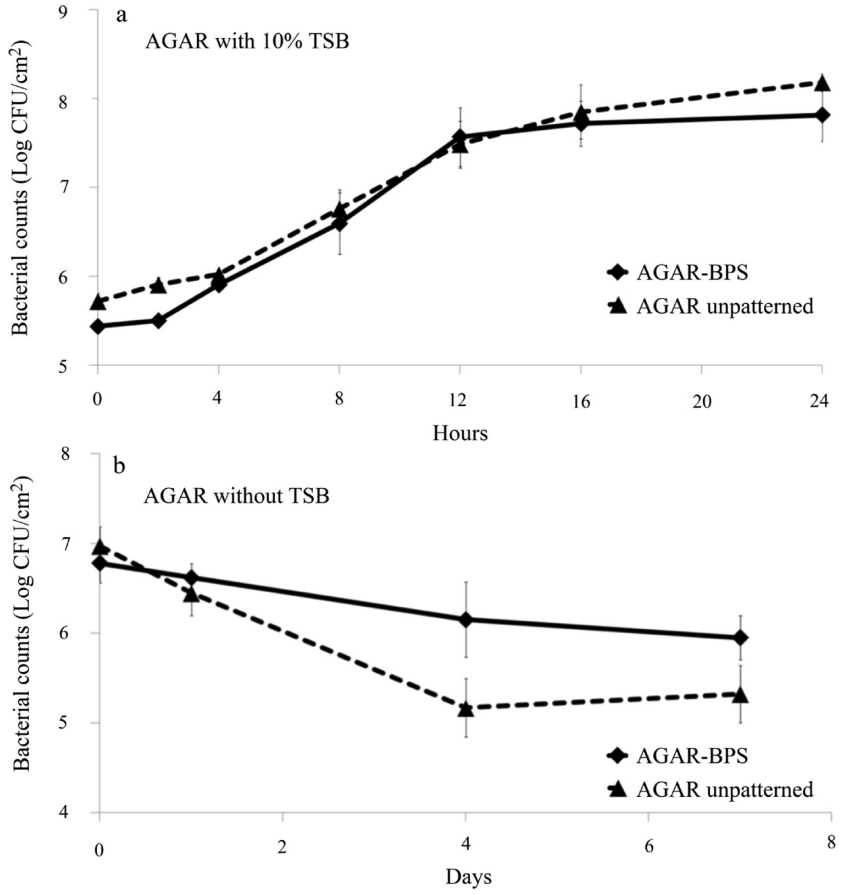

Figure 5. Effect of topography on bacterial growth and survival: (a) bacterial growth on unpatterned and AGAR-BPS with 10% TSB supplement; (b) bacterial survival on AGAR surface without TSB supplement.

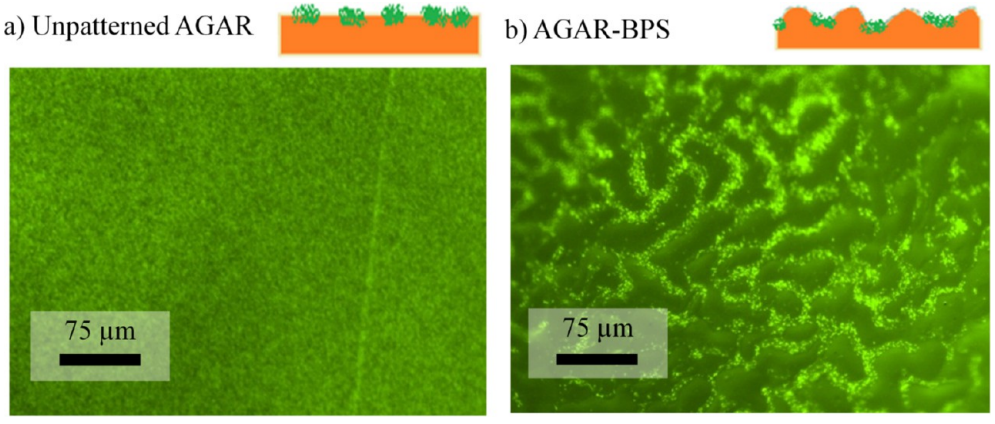

Figure 6. Fluorescence images (100×) of live (green) stained *E. coli* growth on AGAR surface showing effects of topography on bacterial growth: (a) unpatterned AGAR surface after 6 h incubation; (b) AGAR-BPS after 6 h incubation.

biointerface-related research offered by coupling these approaches to biodegradable BPS.

Creating a BPS that supports bacterial growth could facilitate our understanding of how bacteria attach, proliferate, and migrate on complex plant surfaces. We used AGAR-BPS as the substratum to investigate how natural topography and nutrient level affect growth and survival of bacterial cells. Growth of *E. coli* on an unpatterned AGAR surface was compared with that on AGAR-BPS, both with 10% tryptic soy broth (TSB) supplements (Figure 5a). Traditional plate counting, which integrates over the surface, showed no significant difference between patterned and unpatterned surfaces. However, plate counting does not provide spatial distribution information on patterned surfaces. Panels a and b in Figure 6 show the distribution of bacteria on unpatterned AGAR and AGAR-BPS, respectively, after 6 h of incubation. As in the SEM experiments, the inherent heterogeneity of surface topography on the AGAR-BPS leads to a nonuniform distribution of bacterial cells, with localized zones of aggregation in the valleys.[8,26] These results show that AGAR-BPS are compatible with bacterial growth (Figure 5), which can be monitored by traditional culture methods used to evaluate bacterial viability.

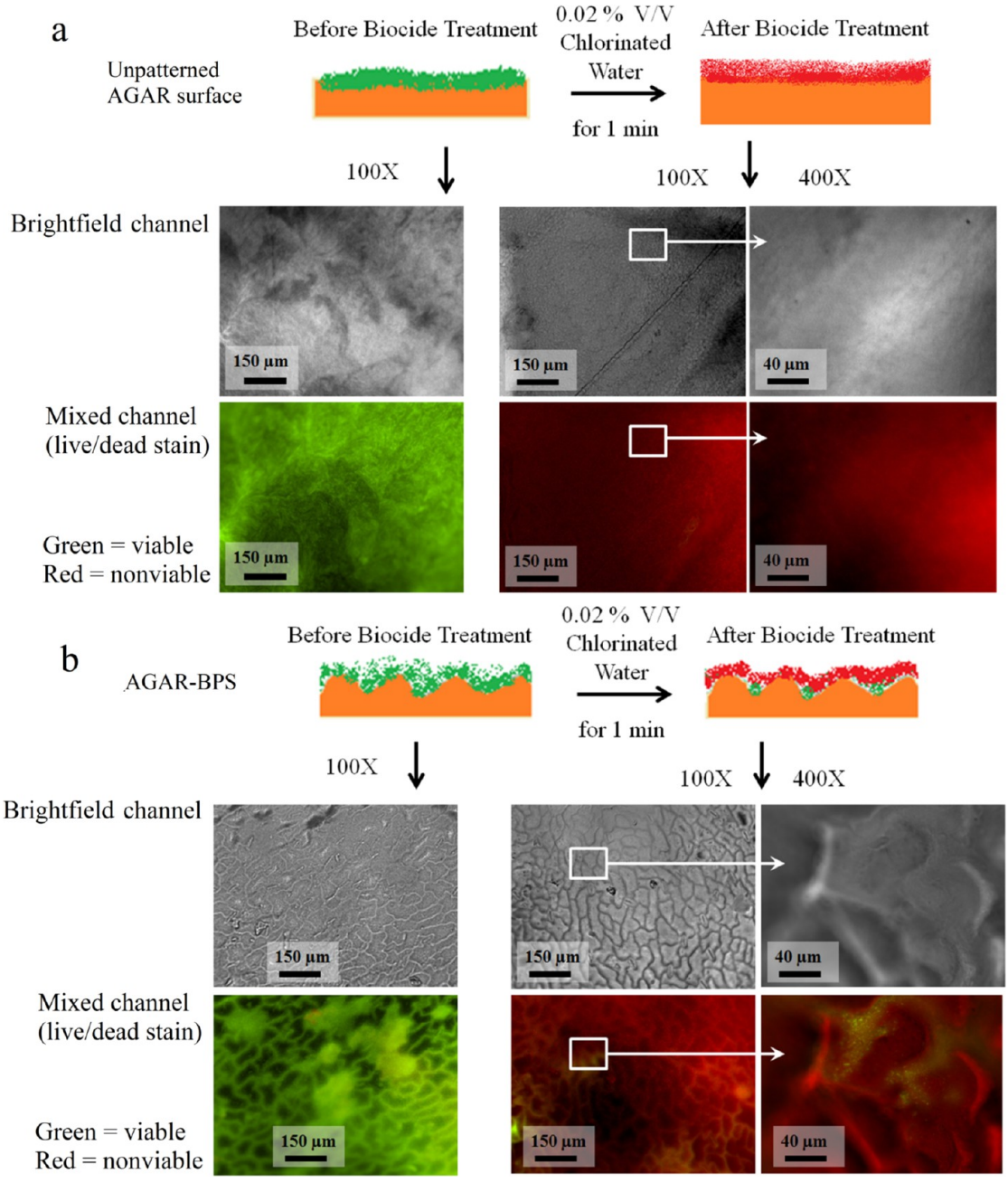

Figure 7. Effect of topography on *E. coli* survival and inactivation during a biocide treatment with 200 mg/L free chlorine for 1 min: (a) unpatterned AGAR surface; (b) AGAR-BPS. The surfaces were subjected to Live/Dead bacterial stain before and after biocide treatment. Green and red indicate live and dead bacteria, respectively.

More importantly, this approach provides the opportunity to study how topographical structure affects bacterial growth and spatial distribution of bacterial cells.

Several recent studies[8,9] suggest that microstructures on plant tissue surfaces provide an environment for bacteria to grow and persist, sheltered from biotic and abiotic stressors. Protection of bacteria by and within the topographic features of plant surface microstructures can significantly reduce the efficacy of various control measures. To date, however, little visualization or understanding of such effects has been possible. Here, we use AGAR-BPS to support formation of bacterial aggregates, and then determine the effects of surface topography on bacterial survival in response to dehydration and biocide treatments.

Nutrient supplementation of AGAR supports bacterial growth, which allows investigation of bacterial survival on patterned surfaces. Figure 5b shows that no later than the fourth day, bacterial survival on AGAR-BPS significantly exceeds survival on an unpatterned AGAR surface. These results indicate that the niches on AGAR-BPS (e.g., replicated valleys and stomatal structures) can offer significant protection to bacterial cells against dehydration. A similar result was previously reported for real plant tissue.[8]

Similarly, BPS can also be used to study how the topography of plant surfaces influences the efficacy of biocide treatment. On an unpatterned AGAR surface (Figure 7a), a relatively thick bacterial growth covered the surface uniformly before biocide treatment. Treatment with chlorinated water (200 mg/L for 1

min) killed most of the bacterial cells, and no viable cells were observed in the enlarged images in Figure 7a. However, on AGAR-BPS (Figure 7b) before biocide treatment, individual bacterial cells are strongly clustered in the valleys, with larger aggregates along the ridges. After biocide treatment with chlorinated water, most bacterial cells were killed. The cell aggregates were no longer observed and the background was covered with red fluorescence, likely due to lysis of bacterial cells during chlorine treatment. Viable cells were still observed in the valleys; a result that can be attributed to the "steric" protection afforded to bacterial aggregates against biocide treatment.[8] The enlarged images in Figure 7b also show a few surviving bacterial cells. Besides providing information on surface topography and bacterial cell viability, AGAR-BPS can also be used for flow cytometry after enzymatic degradation, as shown schematically in Figure 1c. Results shown in Table 1

Table 1. Effects of Surface Topography on Bacterial Survival Determined by Flow Cytometry

	cell counts (log cell/cm^2)[a]			
	unpatterned AGAR surface		AGAR-BPS	
	before biocide treatment	after biocide treatment	before biocide treatment	after biocide treatment
viable counts	7.92 ± 1.01	4.42 ± 0.91	8.52 ± 1.25	6.11 ± 0.75
dead counts	5.36 ± 1.12	7.60 ± 0.88	6.40 ± 0.63	8.31 ± 1.21
reduction of viable counts	3.80 ± 0.85		2.12 ± 0.67	

[a]Log cell counts are shown as mean ± standard error.

indicate that biocide treatment has significantly different outcomes for bacterial inactivation on unpatterned surfaces and AGAR-BPS, as expected. The biocide provides approximately 3.80 vs 2.12 $\log_{10}$ reduction in viable counts on the unpatterned and patterned surfaces, respectively. Similar differential inactivation of pathogens has also been reported with real plant tissues having different surface topographies.[8] Therefore, bactericidal efficacy on BPS is lower than on chemically identical unpatterned surfaces, suggesting that topography provides "steric" protection to bacterial cells. The results also suggest the potential to combine topographical and spatial distribution information using BPS (e.g., SEM and fluorescence microscopy) and downstream flow cytometry detection.

The 3D distribution of bacterial cells (viable and nonviable) was also investigated by orthographic projection from Z-stack measurements using confocal microscopy. Figure 8a shows the orthographic projections of viable bacterial aggregates on AGAR-BPS before biocide treatment. In the X-Y projection, aggregates of viable bacterial cells were observed, consistent with Figure 7a. The X-Z and Y-Z projections show nearly uniform distributions of bacterial cells in the Z direction. After biocide treatment, most of the cells were dead (Figure 8b), and bacterial aggregates were no longer observed in the X-Y projection. Isolated viable cells were observed in the *Z*-axis in X-Z and Y-Z projections, with some in areas corresponding to valleys. This distribution strongly suggests that AGAR-BPS can provide information on how topographical features influence survival of bacterial cells.

MATERIALS AND METHODS

Materials and Chemicals. All chemicals and buffers were purchased from Sigma-Aldrich (St. Louis, MO, USA), except for: SU-8 2050 photoresist and developer (MicroChem, Newton, MA, USA); Sylgard 184 elastomer kit (PDMS) (Dow Chemical Company, Midland, MI, USA); and agarose gel-digesting enzyme GELase (Epicenter Biotechnologies, Madison, WI, USA). Bacterial viability was determined using a Live/Dead *Bac*Light kit (Invitrogen, Grand Island, NY, USA). Fresh spinach leaves (*Spinacia oleracea*) were purchased from a local produce wholesale market (Jessup, Md., USA). The *E. coli* cell-harboring plasmid bearing pRSET/BFP (BFP-*E. coli*) was provided by the Fischell Department of Bioengineering, University of Maryland (College Park, MD, USA).

Replica Molding of PDMS Stamps. For either PDMS or AGAR, BPS were prepared in two steps. The first step was to produce a PDMS stamp with reversed microstructure via replica molding. The second step involved thermal molding of PDMS- and AGAR-BPS from the PDMS molds (Figure 1). To prepare the PDMS molds, spinach leaves were securely taped to the bottom of a 100 mm (ID) aluminum dish. The PDMS mixture (50 g; base:curing agents =10:1) was cast in the dish, followed by degassing in low vacuum for 15 min and curing at 40 °C for 12 h. (The low curing temperature avoids thermal damage to plant tissue.) Cured PDMS stamps were then chemically modified with a layer of Pd nanoparticles (serving as a nonadhesive layer in the thermal molding step) as described below (see Figure 1a).[18,20,27] The PDMS stamps were first oxidized for 10 min in an aqueous solution containing 5.2% (v/v) hydrochloric acid (HCl) and 4.3% (v/v) hydrogen peroxide (H_2O_2) while subjected to ultrasonic treatment (35 kHz), followed by rinsing with H_2O and 100% ethanol. The PDMS stamps were then treated with ultrasound for 45 min in an ethanolic solution (50%, v/v) of (3-aminopropyl) triethoxysilane (APTES) at 22 °C, followed by rinsing in ethanol and H_2O.[18,27] The silylamine-modified PDMS was then shaken overnight at 120 rpm in 0.2 g/L of $PdCl_2$ in 0.2 N HCl aqueous solution, followed by 1 h treatment with 2 g/L NaH_2PO_2 aqueous solution to form the nonadhesive layer of Pd^0 nanoparticles (Figure 1a). The Pd-coated PDMS molds were reusable, and were stored at 4 °C after each thermal molding process.

Thermal Molding of PDMS and AGAR Biomimetically Patterned Surfaces. The PDMS- and AGAR-BPS were prepared from PDMS molds via thermal molding. The PDMS-BPS were molded and cured at 125 °C for 20 min following the manufacturer's protocol (Figure 1b). Replication of AGAR-BPS was achieved by first dissolving 2.5% (w/v) agarose (Type I–B) in water, or in 10% TSB containing 15 g/L tryptone, 5g/L soytone, and 5 g/L NaCl (Figure 1c). Immediately after sterilization, 15 mL of hot liquid medium was cast on PDMS molds (preheated at room temperature and sterilized by 100% ethanol), followed by immediate low-vacuum degassing for 10 s, and transfer to (and rapid gelling in) an ice bath for 5 min. After solidification, the AGAR-BPS was collected and the PDMS mold was recovered.

Bacterial Culture. The BFP-*E. coli* bearing pRSET/BFP plasmid was inoculated into TSB from a frozen stock culture, and incubated for 24 h at 37 °C.[28,29] Cells were harvested by centrifugation at 6000 g for 10 min at 4 °C, followed by two pellet rinses with sterile phosphate buffered saline (PBS). After resuspension and dilution in PBS, each aliquot was determined to contain approximately 1×10^7 CFU/mL of bacterial cells.[8,30]

The bacterial attachment assays on PDMS- and AGAR-BPS were accomplished by inoculating 100 μL of the suspension containing BFP-*E. coli* over a 1 cm^2 area. For PDMS-BPS assays, inocula were dried and incubated for 12 h at 37 °C, and the surface was gently rinsed with PBS for 30 s to remove loosely attached bacterial cells before further characterization. For bacterial growth studies, inoculated AGAR containing 10% TSB was incubated at 25 °C. Growth was examined by traditional plate counting as previously described[8,30−32] and by fluorescence microscopy, at 2-h intervals for 24 h. To study bacterial survival, inoculated AGAR without nutrient supplements was incubated at 4 °C, and plate counts were recorded at 0, 1, 4, and 7

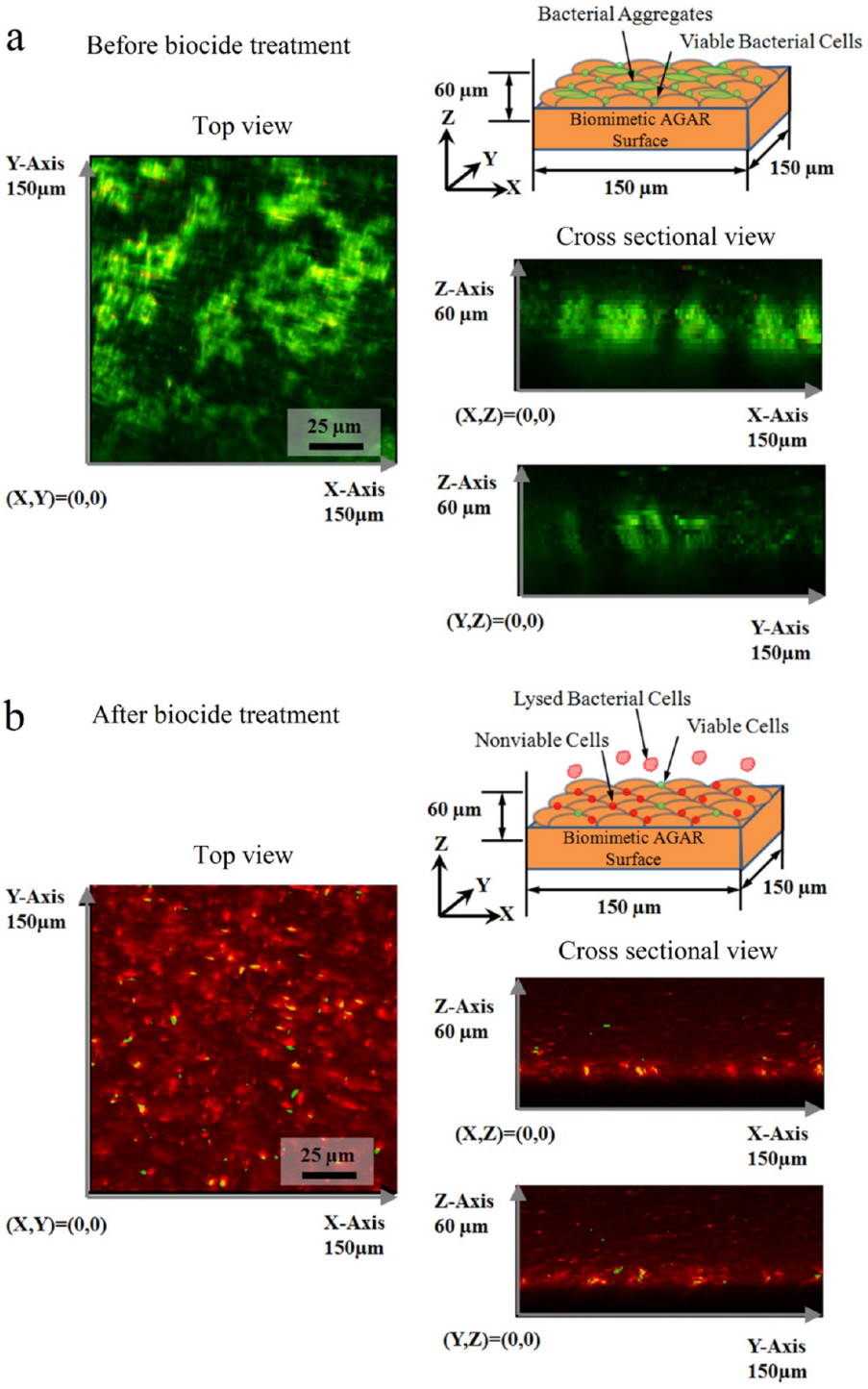

Figure 8. Images illustrating "steric" protection of bacteria in valleys on AGAR-BPS: (a) fluorescent orthographic projection (400 ×) of *E. coli* growth and bacterial aggregates formation after 12 h of incubation; (b) fluorescent orthographic projection (400 ×) of *E. coli* survival after biocide treatment.

days. Before each microscopic observation, bacteria on the AGAR surface were stained at 22 °C for 15 min in the dark with 500 μL of the Live/Dead bacterial viability stain. Buffer containing 6 μM SYTO 9 stains live cells green and 30 μM propidium iodide stains dead cells red. After 12 h of incubation, biocide (200 mg/L chlorinated water) was applied to the surface for 1 min. The bactericidal effect was also examined using the bacterial viability staining kit.

Microscopy. Analyses of surface topography, roughness, and 3D imaging of spinach leaf, PDMS molds, PDMS-BPS, and AGAR-BPS were performed using a 3D digital optical microscope (Hirox KH-7700, Hackensack, NJ, USA). Specimen preparation of PDMS molds and PDMS-BPS was as previously described in the thermal molding section. AGAR-BPS were prepared by molding the sample between the PDMS mold and a glass slide, in order to limit the gel thickness to 1.5 mm and thus reduce light scattering. The magnification power was 1050× using an OL-350 II objective lens, with 3D rendering of surface topography achieved by obtaining several image stacks ranging between 0 and 50 μm at different elevations (1.5 μm/slide) using a motorized Z-axis control. The resolution on the X- and Y-axes was 0.183 μm/pixel, over an area of 300 μm by 200 μm (1.92 million pixels

in total). The data were processed with the manufacturer's 3D profilometry software (Hirox KH-7700 3D Viewer) to generate 3D structural models. R_{RMS} values were calculated from the standard deviation of the z-values of all pixels.

Electron microscopy images were captured utilizing a S-3700 VP-SEM (Hitachi High Technologies America, Inc., Pleasanton, CA, USA) with a Deben Coolstage Peltier stage (Deben UK Ltd., Suffolk, UK) set at −25 °C.[9] Spinach leaves and PDMS-BPS were cut into small pieces before mounting on 51 mm aluminum specimen stubs using conductive carbon tape. All images were captured at 1000× magnification at 10 kV accelerating voltage, 10 mm working distance, and 40 Pa vacuum level.

Fluorescent images for on-chip BFP-*E. coli* or AGAR Live/Dead cell staining were observed and captured using an optical microscope (Nikon E400, Nikon Instruments, Melville, NY, USA) with a fluorescent illuminator (Intensilight C-HGFI, Nikon) and fluorescent filter cubes of BFP, FITC (SYTO 9), and TRITC (for propidium iodide). A Cool Snap HQ camera (Photometrics, Tucson, AZ, USA) and NIS Elements software (version 3.0, Nikon) were used to visualize fluorescent signals. Nikon Plan 10×/0.25 and Nikon Plan 40×/0.65 objective lenses, and a 10× ocular lens were used in the study.[6]

Confocal scanning microscopy (Zeiss LSM-700, Jena, Germany) was used to study the role of surface topography on bacterial growth and survival.[9] The Z-stack function was used to scan a 150 μm × 150 μm area at *Z*-axis resolution of 2 μm/slice. The excitation laser had a wavelength of 488 nm, and a FITC filter was used to capture the SYTO 9 signal (green fluorescence), while a PI filter was used for propidium iodide stained cells (red fluorescence). An EC Plan-Neofluar 40×/0.9 was used as the objective lens. Z-stack images were analyzed and constructed using Zen software (2012, Zeiss).

Contact Angle Measurement. Contact angle measurements were made by the sessile drop method using an Attension Theta optical tensiometer system (Biolin Scientific, Linthicum Heights, MD, USA), with a drop volume of 50 μL (5 drops on a 1 cm × 10 cm strip). Placement of drops of either water, or an aqueous solution of Triton X-100 or Na-CMC, on each surface was controlled by an automatic liquid dispenser (C201, Biolin Scientific). Data recording (60 fps) was triggered by the initial contact of a liquid drop with a solid surface (i.e., an unpatterned PDMS surface, PDMS-BPS, or spinach leaf). We selected leaf portions with relatively low gross curvature, which were quite flat on the scale of the relatively large drops (equivalent spherical diameter of ∼4.6 mm, and equivalent hemispherical diameter of ∼5.8 mm). For each surface type, 20 specimens were used. All measurements were performed with sessile "advanced" drops (i.e., static drops for which the contact surface had most recently advanced), under ambient conditions. Captured images were analyzed automatically (OneAttension software, Version 1.8, Biolin Scientific, Linthicum Heights, MD, USA) to identify the baseline and calculate contact angles.

Flow Cytometry. Flow downstream of the AGAR-BPS (Figure 1c) was quantified with a flow cytometer to demonstrate the possibility of counting cells and monitoring their viability.[33] After microscopic examination, AGAR-BPS (1 cm^2) were enzymatically degraded in 10 mL of GELase solution (20 units/mL) at 45 °C for 40 min. Aliquots of 1 mL of the resulting suspension containing live and dead bacterial cells were then analyzed by flow cytometry (FACS Canto II, BD Biosciences, San Jose, CA, USA) for fluorescence expression and viability counts. The negative control was prepared using a bacterial suspension of cells grown on an unpatterned AGAR surface, and sterilizing the suspension with 200 mg/L chlorinated water for 1 min. Flow cytometry data were analyzed by FACS Canto clinical software (BD Biosciences, Sparks, MD) to calculate means and standard errors of cell counts and survival rates.

Statistical Analysis. Surface roughness, contact angle, and flow cytometry experiments were conducted with five replications, and the data were reported as mean ± standard error. Analysis of variance (ANOVA) was performed using SAS software (Version 9.2, SAS Institute Inc., Cary, NC). Surface roughness of PDMS molds and BPS were tested against that of spinach leaf by ANOVA Dunnett's test. The contact angles of water, and of the aqueous solutions of Triton X-100 and Na-CMC, on unpatterned PDMS, PDMS-BPS, and spinach leaves were ranked using ANOVA Tukey's test. The probability (P) of all test statistics was set at 0.05.

■ COMMENTS AND CONCLUSIONS

In this study, a two-step replica molding method was developed for rapid fabrication of polymer-based biomimetically patterned surfaces (BPS) having the surface microstructure of plant tissue. Surfaces of PDMS- and AGAR-BPS replicating spinach leaf microstructure demonstrate a high degree of topographical fidelity to the original plant tissue. PDMS surfaces provide structural stability under vacuum for SEM-associated applications, and have surface wettability similar to natural leaf surfaces, which will facilitate development of coating and biocide-related intervention technologies. The possibility of chemically functionalizing PDMS[27] allows for potential tailoring of chemical properties important to bacterial attachment, with independent control of microstructural topography. For AGAR surfaces, simple adjustment of nutrient levels facilitates investigation of how natural topography affects bacterial growth and survival. Exploratory experiments show that high-fidelity topography, structural stability, and the capability to integrate with instrumentation for studying bacterial growth and survival on PDMS- and AGAR-BPS, provide potentially valuable tools for plant−bacteria interaction studies, including those relevant to food safety. AGAR-BPS can also be enzymatically degraded to recover bacterial cells for subsequent studies using flow cytometry and other microbial detection and enumeration technologies. For AGAR-BPS, the ease with which composition is modifiable provides the opportunity to independently study the effects of surface chemistry, microstructure, and nutrients on bacterial attachment, growth, and survival for a wide variety of bacteria.

Surfaces with simple, spatially periodic microstructures in which each feature has a high degree of symmetry can be extremely useful for understanding certain basic mechanisms of attachment. However, their use as testbeds for studying the details of surface interactions (including attachment and detachment) for specific bacteria/plant pairs, and in the evaluation and optimization of sanitization techniques and other postharvest treatments, is severely limited by the lack of geometric complexity. Real plant surfaces are highly complex at the micro- and nanoscale, and so the value of an approach that provides for reproducible studies of geometrically complex surfaces is evident. A key advantage of the present approach is that it avoids two pitfalls of conventional microfabrication techniques for producing geometrically complex surfaces. First, existing approaches require laborious clean-room fabrication processes involving multiple high-vacuum (e.g., ion sputter coating) and high-temperature (e.g., nickel stamp electroplating at 55−70 °C) treatments.[34−36] Second, those methods reproduce plant surface structures on a self-cleaning superhydrophobic surface, which is generally incompatible with cellular attachment.[34,36,37] An additional advantage of the present approach is that it allows for a relatively "clean" separation of the effects of surface microstructure from those of surface chemistry and nanoscale texturing, since one can independently control the chemical composition and properties of the polymeric surface, while maintaining identical microstructures in the replica molding process.

Initial applications tested in this study demonstrate the robustness of biomimetically patterned surfaces and their potential application to other areas of plant or animal tissue-

microbe interface research. Because surface biochemistry is also critical to bacterial attachment, growth, and inactivation, establishing biochemical similarity would be the next step. Systematic evaluation of the interaction between living bacterial cells and surfaces is essential to development of possible interventions directed at reducing or eliminating attachment and microbial survival. Although spinach leaves were chosen as the plant surface in this study, the method developed has great potential for replicating the surfaces of other plant and animal tissues. We anticipate that this approach will provide an important research tool for understanding surface−bacteria interactions and facilitating development of technology to enhance inactivation of foodborne human pathogens and improve public health.

AUTHOR INFORMATION

Corresponding Author

*E-mail: yaguang.luo@ars.usda.gov. Tel: 301.504.6186. Fax: 301.504.5107.

Notes

The authors declare no competing financial interest.

ACKNOWLEDGMENTS

This work was supported by USDA-NIFA Specialty Crop Research Initiative Grant Award 2010-01165. We also acknowledge grant HDTRA1-13-0037 and BO085PO008 from the U.S. Defense Threat Reduction Agency. We are grateful for the support of the FabLab at the Maryland NanoCenter. We thank Dr. William Bentley and Ms. Jessica Terrell of the Fischell Department of Bioengineering at the University of Maryland, College Park, for providing BFP-*E. coli* strains and for generous technical support. Access to the FACS equipment at the Flow Cytometry Core Facility (Maryland Pathogen Research Institute, University of Maryland) is gratefully acknowledged.

REFERENCES

(1) CDC, CDC Estimates of Foodborne Illness in the United States 2011, CS218786-A.

(2) Lynch, M. F.; Tauxe, R. V.; Hedberg, C. W. The Growing Burden of Foodborne Outbreaks due to Contaminated Fresh Produce: Risks and Opportunities. *Epidemiol. Infect.* **2009**, *137*, 307−315.

(3) Erickson, M. C. Internalization of Fresh Produce by Food borne Pathogens. *Annu. Rev. Food Sci. Technol.* **2012**, *3*, 283−310.

(4) Erickson, M. C.; Webb, C. C.; Diaz-Perez, J. C.; Davey, L. E.; Payton, A. S.; Flitcroft, I. D.; Phatak, S. C.; Doyle, M. P. Internalization of *Escherichia coli* O157:H7 Following Spraying of Cut Shoots when Leafy Greens are Regrown for a Second Crop. *J. Food Prot.* **2013**, *76*, 2052−2056.

(5) Erickson, M. C.; Webb, C. C.; Diaz-Perez, J. C.; Davey, L. E.; Payton, A. S.; Flitcroft, I. D.; Phatak, S. C.; Doyle, M. P. Absence of Internalization of *Escherichia coli* O157:H7 into Germinating Tissue of Field-Grown Leafy Greens. *J. Food Prot.* **2014**, *77*, 189−196.

(6) Sharma, M.; Ingram, D. T.; Patel, J. R.; Millner, P. D.; Wang, X.; Hull, A. E.; Donnenberg, M. S. A Novel Approach to Investigate the Uptake and Internalization of *Escherichia coli* O157:H7 in Spinach Cultivated in Soil and Hydroponic Medium. *J. Food Prot.* **2009**, *72*, 1513−1520.

(7) Whitehead, K. A.; Verran, J. The Effect of Surface Topography on the Retention of Microorganisms. *Food Bioprod. Process.* **2006**, *84*, 253−259.

(8) Wang, H.; Feng, H.; Liang, W.; Luo, Y.; Malyarchuk, V. Effect of Surface Roughness on Retention and Removal of *Escherichia coli* O157:H7 on Surfaces of Selected Fruits. *J. Food Sci.* **2009**, *74*, E8−E15.

(9) Macarisin, D.; Patel, J.; Bauchan, G.; Giron, J. A.; Ravishankar, S. Effect of Spinach Cultivar and Bacterial Adherence Factors on Survival of *Escherichia coli* O157:H7 on Spinach Leaves. *J. Food Prot.* **2013**, *76*, 1829−1837.

(10) Seo, K. H.; Frank, J. F. Attachment of *Escherichia coli* O157:H7 to Lettuce Leaf Surface and Bacterial Viability in Response to Chlorine Treatment as Demonstrated by Using Confocal Scanning Laser Microscopy. *J. Food Prot.* **1999**, *62*, 3−9.

(11) Warning, A.; Datta, A. K. Interdisciplinary Engineering Approaches to Study How Pathogenic Bacteria Interact with Fresh Produce. *J. Food Eng.* **2013**, *114*, 426−448.

(12) Apoga, D.; Barnard, J.; Craighead, H. G.; Hoch, H. C. Quantification of Substratum Contact Required for Initiation of *Colletotrichum graminicola* Appressoria. *Fungal Genet. Biol.* **2004**, *41*, 1−12.

(13) Held, M.; Edwards, C.; Nicolau, D. V. Probing the Growth Dynamics of *Neurospora crassa* with Microfluidic Structures. *Fungal Biol.* **2011**, *115*, 493−505.

(14) De la Fuente, L.; Montanes, E.; Meng, Y. Z.; Li, Y. X.; Burr, T. J.; Hoch, H. C.; Wu, M. M. Assessing Adhesion Forces of Type I and Type IV Pili of *Xylella fastidiosa* Bacteria by Use of a Microfluidic Flow Chamber. *Appl. Environ. Microbiol.* **2007**, *73*, 2690−2696.

(15) Sirinutsomboon, B.; Delwiche, M. J.; Young, G. M. Attachment of *Escherichia coli* on Plant Surface Structures Built by Microfabrication. *Biosyst. Eng.* **2011**, *108*, 244−252.

(16) Friedlander, R. S.; Vlamakis, H.; Kim, P.; Khan, M.; Kolter, R.; Aizenberg, J. Bacterial Flagella Explore Microscale Hummocks and Hollows to Increase Adhesion. *Proc. Natl. Acad. Sci. U.S.A.* **2013**, *110*, 5624−5629.

(17) Seo, J.; Lee, L. P. Effects on Wettability by Surfactant Accumulation/Depletion in Bulk Polydimethylsiloxane (PDMS). *Sens. Actuators, B* **2006**, *119*, 192−198.

(18) Zhang, B.; Feldman, A.; Wang, Q. A Novel Insight in Rapid Allergen Detection in Food Systems: from Threshold Dose to Real-World Concentration. *Sens Actuators, B* **2013**, *186*, 597−602.

(19) Anselme, K.; Davidson, P.; Popa, A. M.; Giazzon, M.; Liley, M.; Ploux, L. The Interaction of Cells and Bacteria with Surfaces Structured at the Nanometre Scale. *Acta Biomater.* **2010**, *6*, 3824−3846.

(20) McDonald, J. C.; Duffy, D. C.; Anderson, J. R.; Chiu, D. T.; Wu, H. K.; Schueller, O. J. A.; Whitesides, G. M. Fabrication of Microfluidic Systems in Poly(dimethylsiloxane). *Electrophoresis* **2000**, *21*, 27−40.

(21) Feng, L.; Zhang, Y. A.; Xi, J. M.; Zhu, Y.; Wang, N.; Xia, F.; Jiang, L. Petal Effect: a Superhydrophobic State with High Adhesive Force. *Langmuir* **2008**, *24*, 4114−4119.

(22) Hall-Stoodley, L.; Costerton, J. W.; Stoodley, P. Bacterial Biofilms: from the Natural Environment to Infectious Diseases. *Nat. Rev. Microbiol.* **2004**, *2*, 95−108.

(23) Debeer, D.; Stoodley, P.; Roe, F.; Lewandowski, Z. Effects of Biofilm Structures on Oxygen Distribution and Mass-Transport. *Biotechnol. Bioeng.* **1994**, *43*, 1131−1138.

(24) Huang, C. T.; Xu, K. D.; McFeters, G. A.; Stewart, P. S. Spatial Patterns of Alkaline Phosphatase Expression within Bacterial Colonies and Biofilms in Response to Phosphate Starvation. *Appl. Environ. Microbiol.* **1998**, *64*, 1526−1531.

(25) Rizzello, L.; Sorce, B.; Sabella, S.; Vecchio, G.; Galeone, A.; Brunetti, V.; Cingolani, R.; Pompa, P. P. Impact of Nanoscale Topography on Genomics and Proteomics of Adherent Bacteria. *ACS Nano* **2011**, *5*, 1865−1876.

(26) Lawrence, J. R.; Korber, D. R.; Hoyle, B. D.; Costerton, J. W.; Caldwell, D. E. Optical Sectioning of Microbial Biofilms. *J. Bacteriol.* **1991**, *173*, 6558−6567.

(27) Yu, L.; Li, C.; Liu, Y. S.; Gao, J.; Wang, W.; Gan, Y. Flow-through Functionalized PDMS Microfluidic Channels with Dextran Derivative for ELISAs. *Lab Chip* **2009**, *9*, 1243−1247.

(28) Tsao, C. Y.; Hooshangi, S.; Wu, H. C.; Valdes, J. J.; Bentley, W. E. Autonomous Induction of Recombinant Proteins by Minimally Rewiring Native Quorum Sensing Regulon of *E. coli*. *Metab. Eng.* **2010**, *12*, 291−297.

(29) Cheng, Y.; Luo, X. L.; Tsao, C. Y.; Wu, H. C.; Betz, J.; Payne, G. F.; Bentley, W. E.; Rubloff, G. W. Biocompatible Multi-Address 3D Cell Assembly in Microfluidic Devices using Spatially Programmable Gel Formation. *Lab Chip* **2011**, *11*, 2316−2318.
(30) Shen, C.; Luo, Y.; Nou, X.; Bauchan, G.; Zhou, B.; Wang, Q.; Millner, P. Enhanced Inactivation of *Salmonella* and *Pseudomonas* Biofilms on Stainless Steel by Use of T-128, a Fresh-Produce Washing Aid, in Chlorinated Wash Solutions. *Appl. Environ. Microb.* **2012**, *78*, 6789−6798.
(31) Zhang, B.; Luo, Y.; Wang, Q. Development of Silver-Zein Composites as a Promising Antimicrobial Agent. *Biomacromolecules* **2010**, *11*, 2366−2375.
(32) Zhang, B.; Luo, Y.; Wang, Q. Development of Silver/Alpha-Lactalbumin Nanocomposites: A New Approach to Reduce Silver Toxicity. *Int. J. Antimicrob. Agents* **2011**, *38*, 502−509.
(33) Gupta, A.; Terrell, J. L.; Fernandes, R.; Dowling, M. B.; Payne, G. F.; Raghavan, S. R.; Bentley, W. E. Encapsulated Fusion Protein Confers "Sense and Respond" Activity to Chitosan-Alginate Capsules to Manipulate Bacterial Quorum Sensing. *Biotechnol. Bioeng.* **2013**, *110*, 552−562.
(34) Lee, S. M.; Kwon, T. H. Mass-producible Replication of Highly Hydrophobic Surfaces from Plant Leaves. *Nanotechnology* **2006**, *17*, 3189−3196.
(35) Lee, S. M.; Upping, J.; Bielawny, A.; Knez, M. Structure-Based Color of Natural Petals Discriminated by Polymer Replication. *ACS Appl. Mater. Interfaces* **2011**, *3*, 30−34.
(36) Liu, B.; He, Y. N.; Fan, Y.; Wang, X. G. Fabricating Superhydrophobic Lotus-leaf-like Surfaces through Soft-lithographic Imprinting. *Macromol. Rapid Commun.* **2006**, *27*, 1859−1864.
(37) Lampin, M.; Warocquier-Clerout, R.; Legris, C.; Degrange, M.; Sigot-Luizard, M. F. Correlation between Substratum Roughness and Wettability, Cell Adhesion, and Cell Migration. *J. Biomed. Mater. Res.* **1997**, *36*, 99−108.